

Supporting Information

The Membrane Environment Drives Cytochrome P450's Spin Transition and its Interaction with Cytochrome b_5

Thirupathi Ravula¹, Carlo Barnaba¹, Mukesh Mahajan¹, G.M. Anantharamaiah², Sang-Choul Im³, Lucy Waskell³, Ayyalusamy Ramamoorthy¹

Experimental section

Materials and Reagents. Phosphate buffer components (potassium phosphate monobasic and dibasic) and benzphetamine were purchased from Sigma-Aldrich (St. Louis, MO). 1,2-dimyristoyl-sn-glycero-3-phosphocholine (DMPC), 1-palmitoyl-2-oleoyl-sn-glycero-3-phosphocholine (POPC) and 1-palmitoyl-2-oleoyl-sn-glycero-3-phospho-L-serine (sodium salt) (POPS) were purchased from Avanti Polar Lipids, Inc. (Alabaster, AL). The amino acid sequence of the 4F peptide used to prepare lipid nanodiscs was **DWFKAFYDKVAEKFKAAF**. Deuterium oxide and ^{15}N Celtone Base Powder was purchased from Cambridge Isotope Laboratories (Tewksbury, MA). The 5-mm symmetrical D_2O -matched Shigemi NMR microtubes were purchased from Shigemi, Inc (Allison Park, PA).

Proteins expression and purification. Full-length uniformly ^{15}N -labeled and unlabeled wild-type *cytb₅* was expressed and purified as described previously.^[1-3] Briefly, *E. coli* C41 cells were transformed with a pLW01 plasmid containing the *cytb₅* gene. The cells were grown in LB medium to an OD of 1 at 600 nm. The culture was diluted 100-fold into 10 mL of ^{15}N -Celtone medium. This culture was grown at 35 °C with shaking at 250 rpm until an OD of 1 at 600 nm was achieved. The cells were pelleted and resuspended in 10 mL of fresh ^{15}N -Celtone medium. The resuspended cell culture was added to the final 1 L of culture minimum medium. Isopropyl β -D-thiogalactopyranoside was added to a final concentration of 10 μM , and incubation was continued for 20 h, at which time the cells were harvested. ^{15}N -labeled cytochrome *b₅* (*cytb₅*) was purified as described previously.^[4] Expression and purification of the cytochrome P450 2B4 (CYP2B4) were performed as described in the literature.^[3,5]

Nanodiscs preparation and characterization. DMPC, POPC and POPS powders were dissolved in HPLC-grade chloroform to make stock solutions at 20 mg/mL. The 4F peptide was dissolved in buffer A (40 mM potassium phosphate, pH 7.4) to make a stock solution at 10mg/mL. Several phospholipid mixtures were obtained: DMPC (100%), POPC (100%), POPC:POPS 8:2 (w/w), POPC:POPS 1:1 (w/w), POPC:POPS 2:8 (w/w), and POPS (100%). For the structural studies, we used DMPC (100%) and POPC:POPS 8:2, this last for being physiologically relevant in terms of negative charged lipids percentage of the mammalian ER.^[6] Aliquots corresponding to the required phospholipid molar ratio were transferred to an Eppendorf vial and dried under gentle flow of N_2 for 3h, followed by a 2h drying step in a desiccator under vacuum. The lipid cake was hydrated with buffer A to get a 10 mg/mL solution and 4F peptide solution was added to a peptide:lipid ratio of 1:1.5 w/w and 1:1 w/w for DMPC and POPC:PS, respectively. The mixture was incubated at 37 °C o/n in slow agitation mode. Empty nanodiscs (ND) were purified by size exclusion chromatography (SEC), using Superdex 200 Increase 300/10 GL column operated on an AKTA purifier (GE Healthcare, Freiburg, Germany). ND characterization was also performed by dynamic light scattering (DLS), on a DynaPro Nanostar equipment (Wyatt Technology Co., Goleta, CA).

CYP2B4:*cytb₅* complex was reconstituted by the two-steps protocol described elsewhere.^[7] Briefly, *cytb₅* was incubated in 4F-ND at 25°C, followed by SEC purification. Then, full length CYP2B4 was incubated overnight with *cytb₅* nanodiscs, followed by the purification of the complex using SEC; mobile phase consisted in 40 mM KPi at pH 7.4. For all the nanodiscs preparation, the size distribution was determined by DLS. Concentration of CYP2B4 in ND was determined based on the CO-spectrum, using an extinction coefficient of $\Delta\epsilon_{450-490} = 91 \text{ mM}^{-1} \text{ cm}^{-1}$.^[8] The concentration of *cytb₅* was using an extinction coefficient of $117 \text{ mM}^{-1} \text{ cm}^{-1}$ at 413 nm.^[9]

Titration of CYP2B4 with benzphetamine. CYP2B4 (10-12 μM) monomerized in nanodiscs was titrated with benzphetamine. Titrations were performed in 10 mM phosphate buffer at 25°C. UV-visible spectra were monitored with a Cary 4000 spectrometer (Agilent Technologies, Santa Clara, CA) between 300 and 750 nm. The analysis of the spectral series was done using a principal component analysis method, followed by least-square (PLS) fitting of the spectra by a set of spectral standards of pure high-spin, low-spin, and P420 species of CYP2B4 (Figure S10).^[10] Spectral analysis and PLS fitting were performed using SpectraLab software package.^[11] The molar fraction in high-spin state was plotted against BP, and curves were fitted to obtain the spectral binding constant (K_S).

Titration of CYP2B4-ND with *cytb*₅. CYP2B4 was reconstituted in ND and concentrated up to 10-12 μM of protein. Titration were performed adding *cytb*₅ in solution, in the presence and absence of saturating concentration (500 μM) of the substrate benzphetamine. *Cytb*₅ was added to both sample and reference cuvettes, in order to take into account only the spectral changes of CYP2B4, as described previously.^[3, 12] UV-visible spectra were monitored with a Cary 4000 spectrometer (Agilent Technologies, Santa Clara, CA) between 300 and 700 nm. The analysis of the spectral series was done as described above using SpectraLab software package.^[11] The molar fraction in high-spin state was plotted against *cytb*₅ equivalents; for all the titration experiments we obtained a sigmoidal plot, which cannot be fitted with a binary equilibrium model.^[3] Thus, the curves were fitted with the following logistic equation:

$$[HS] = \frac{[HS]_0 + ([HS]_{max} - [HS]_0)}{\left(1 + \left(\frac{[cytb_5]}{K_d}\right)^n\right)}$$

Where $[HS]_0$ is the initial high-spin concentration, $[HS]_{max}$ is the maximum high-spin concentration, K_d is the dissociation equilibrium constant and n is a fitting parameter. This equation is analogue to Hill's equation for protein-ligand binding cooperativity, thus n is an estimation of the binding events.

Solution NMR of *cytb*₅-CYP450 Complex. For titration experiments, 100 μM of *cytb*₅ reconstituted in DMPC and POPC-PS 8:2 nanodiscs were recorded, followed by titration with 0.4, 0.8 and 1.2 equivalents of full length CYP2B4. The CYP2B4 stock solutions were exchanged with NMR buffer (40mM KPi with 10% D₂O) at lower concentration (90 μM), and then added to *cytb*₅-containing nanodiscs; the mixture was concentrated to a final volume of 300 μl , so that the final concentration of ¹⁵N-*cytb*₅ remained constant. NMR spectra were recorded at 298K on a Bruker Avance II 600-MHz spectrometer equipped with a cryoprobe. All experiments were recorded using two-dimensional ¹⁵N-¹H TROSY HSQC spectra with 64 scans and 256 t_1 increments. Data was processed using TopSpin 2.0 (Bruker Co., Billerica, MA) and analyzed with Sparky 3.115.^[13] The previously reported *cytb*₅ backbone chemical shift assignments were used in this study.^[14] The weighted amide chemical shift perturbation ($\Delta\delta_{avg}$) was calculated using the following equation:

$$\Delta\delta_{avg} = \sqrt{\left(\Delta\delta N + \frac{F_2 SW}{F_1 SW}\right)^2 + \Delta\delta H^2}$$

Where $\Delta\delta N$ and $\Delta\delta H$ are the changes in the chemical shifts of amide nitrogen-15 and amide-proton respectively, while $F_1 SW$ and $F_2 SW$ represent the spectral width in the first and second dimensions respectively; chemical shift values are given in ppm.

CYP2B4-cyt_b₅ Complex Structure Calculation. The HADDOCK (High Ambiguity Driven protein-protein DOCKing) docking software (v.2.2, Zundert; Wassannar) was used to dock cytb₅ and CYP2B4 and calculate the structures of complex based on experimental ambiguous NMR restraints and site-directed mutagenesis experiments reported in our previous work.^[1] HADDOCK involves rigid body docking, followed by molecular dynamic simulations that allow selected aminoacid side chains, as well as parts of the backbone, to move freely to improve the complementarity and electrostatic interactions at the interface. For this calculation, we used our solution NMR structure of full length rabbit cytb₅ (PDB structure 2M33) and the x-ray structure of the heme domain of CYP2B4 lacking the transmembrane anchor (PDB code 1PO5) Additionally, the ligand bound CYP450 (PDB code 1SUO)^[15] was also used. HADDOCK was run using the default parameters. Ligand topology and parameter files were generated from the PRODRG2 server.^[16] Experimental unambiguous^[3] and ambiguous intermolecular restraints obtained from mutagenesis and NMR data (Table S3) were used in data driven docking simulation. To obtain a high-resolution structural model of the productive complex, the cofactors and ligand were not removed during simulation. Solution NMR identified residues of cytb₅ were included as active restraints (Table S3), whereas the server automatically defined passive residues nearby the interaction site. The active restraints on CYP450 side were selected from earlier published articles.^[1, 3, 17] Rigid body energy minimization was used for docking 1000 structures of the complex. The second step included semi-rigid simulated annealing on which the best 200 structures were further refined with explicit solvent in an 8.0 Å shell of TIP3P water molecules. The 200 lowest energy structures were selected for the final analysis and grouped into two main clusters based on the backbone RMSD.

Stopped-Flow Kinetics. All experiments were performed at 25 °C under anaerobic conditions using a Hi-Tech SF61DX2 stopped-flow spectrophotometer (Bradford-on-Avon, UK) housed in an anaerobic Belle Technology glove box (Weymouth, UK). The buffer was purged with nitrogen gas for 30 minutes for deoxygenation prior to being transferred to the glove box. All protein solutions were incubated overnight at 4 °C in the glove box to eliminate oxygen.

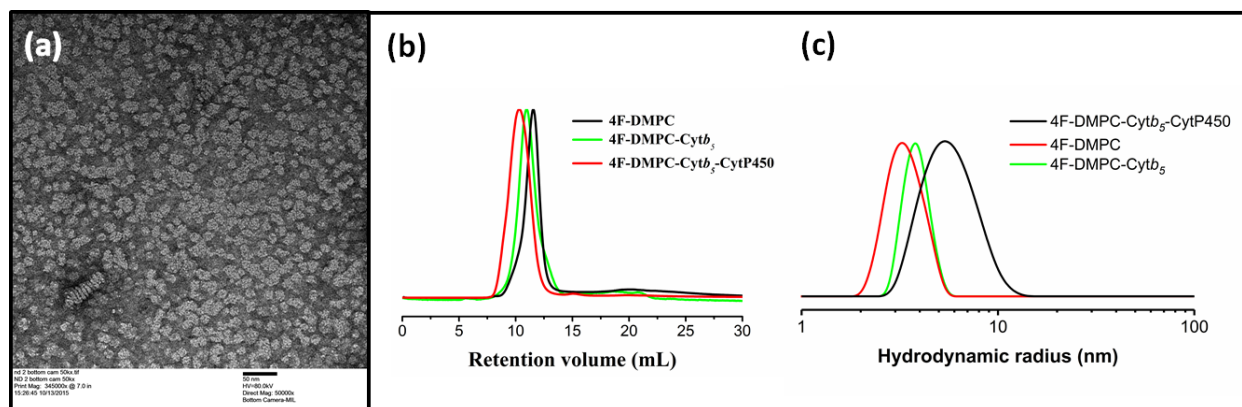


Figure S1. a) TEM image showing disc-shaped empty 4F-DMPC nanodiscs. SEC (b) and DLS (c) characterization of empty 4F-DMPC nanodiscs (black line), and reconstituted with *cytb*₅ (red line) and *cytb*₅-*cytP450* complex (green line).

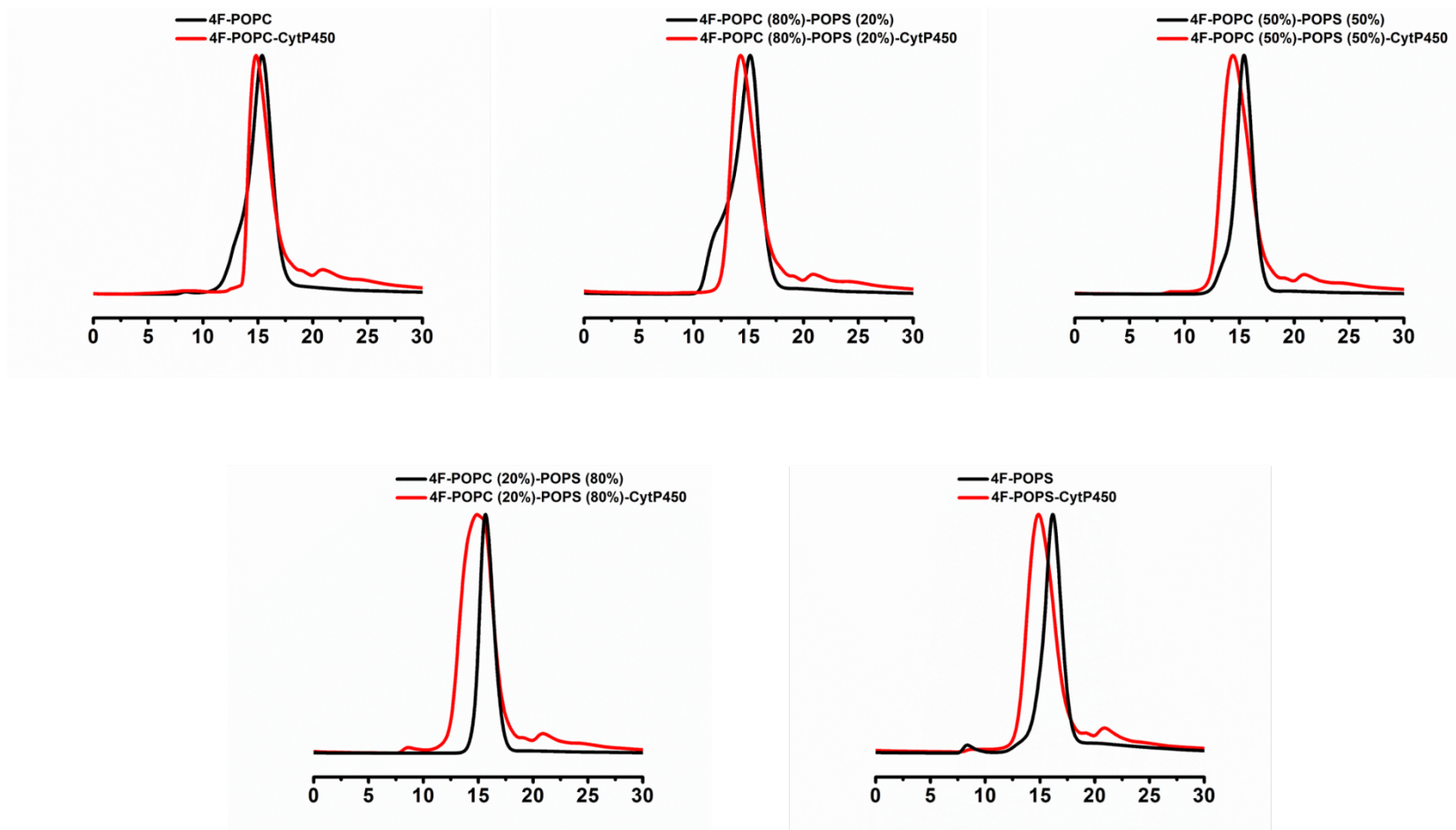


Figure S2. Size exclusion profiles of lipid-nanodiscs without (black) and with reconstituted CytP450 (red) with varying lipid composition. All the nanodiscs were prepared using 1:1 w/w peptide to lipid ratios.

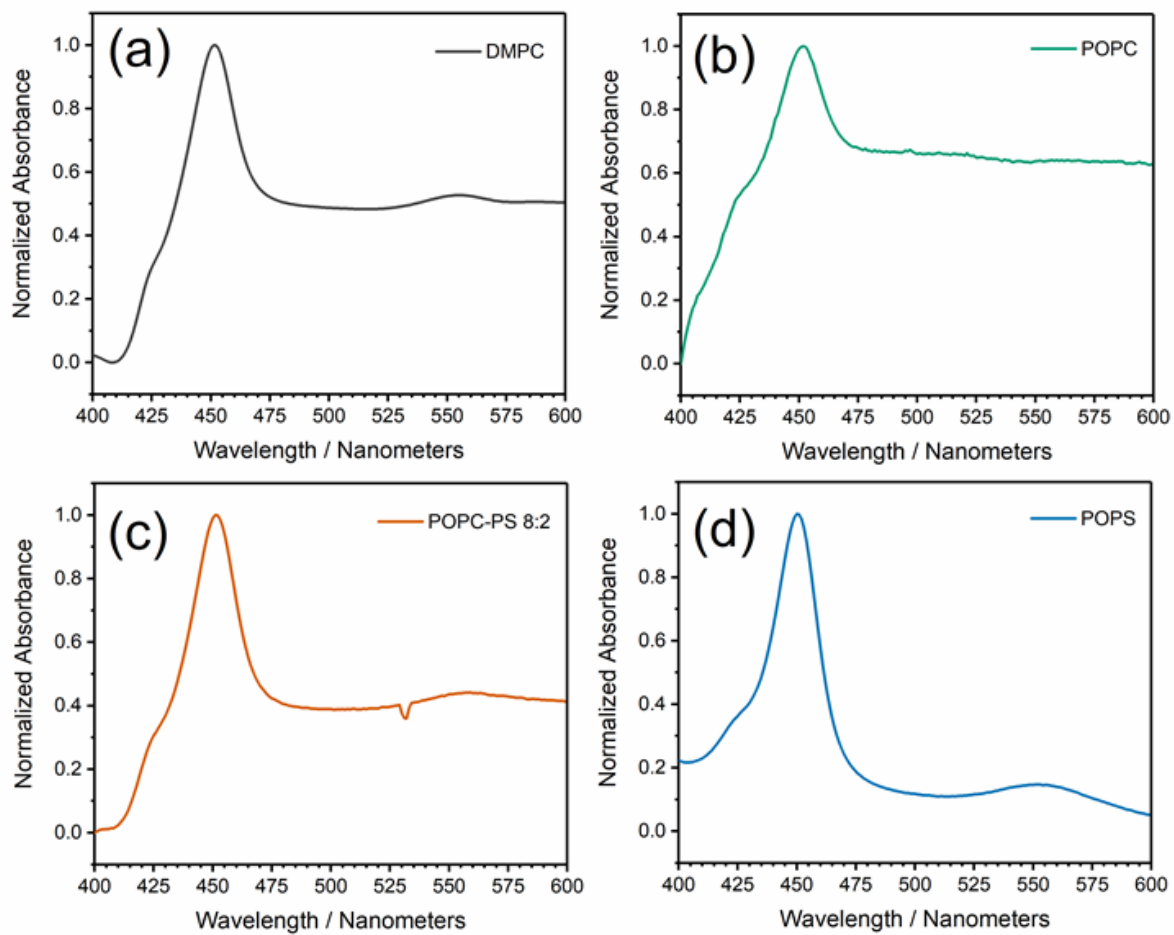


Figure S3. UV-vis absorption spectra of several different 4F-peptide nanodiscs showing CO-bound peak at 450 nm.

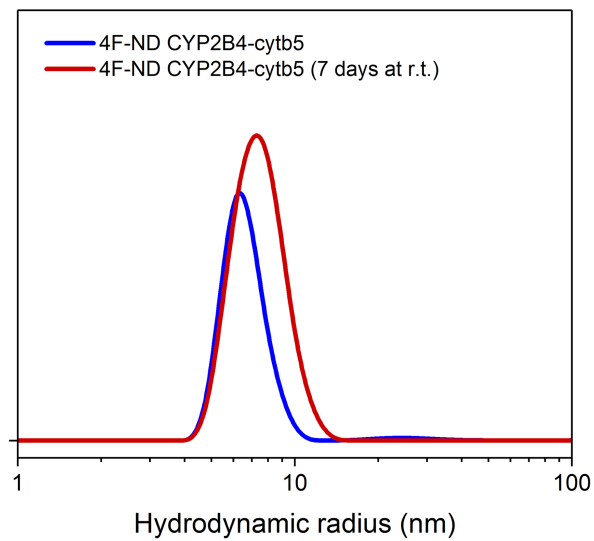


Figure S4. Stability of the CYP2B4-cyt b_5 complex in DMPC 4F-nanodiscs under 40 mM KPi buffer (pH 7.4) measured after purification with SEC. Fresh sample (blue solid line) and sample stored for 7 days at room temperature (red line).

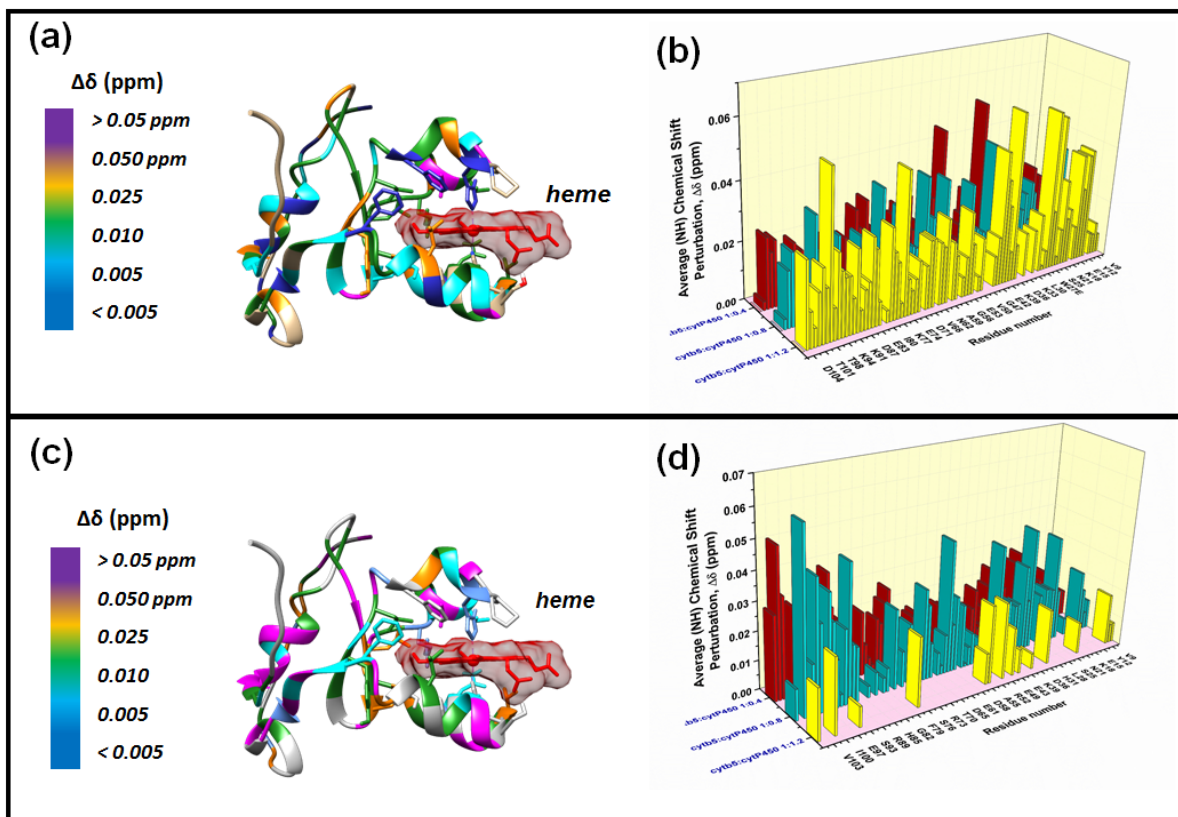


Figure S5. Chemical shifts perturbations ($\Delta\delta$) analysis for *cytb*₅-CYP2B4 complex in DMPC (top) and POPC-PS (8:2) (bottom) 4F-nanodiscs. In a) and c) chemical shifts perturbations for residues in *cytb*₅ upon complex formation with CYP2B4 are represented as continuous color maps on the NMR structure of *cytb*₅ (PBD code 2M33); b) and d) are histograms representing the experimentally measured changes in chemical shifts values.

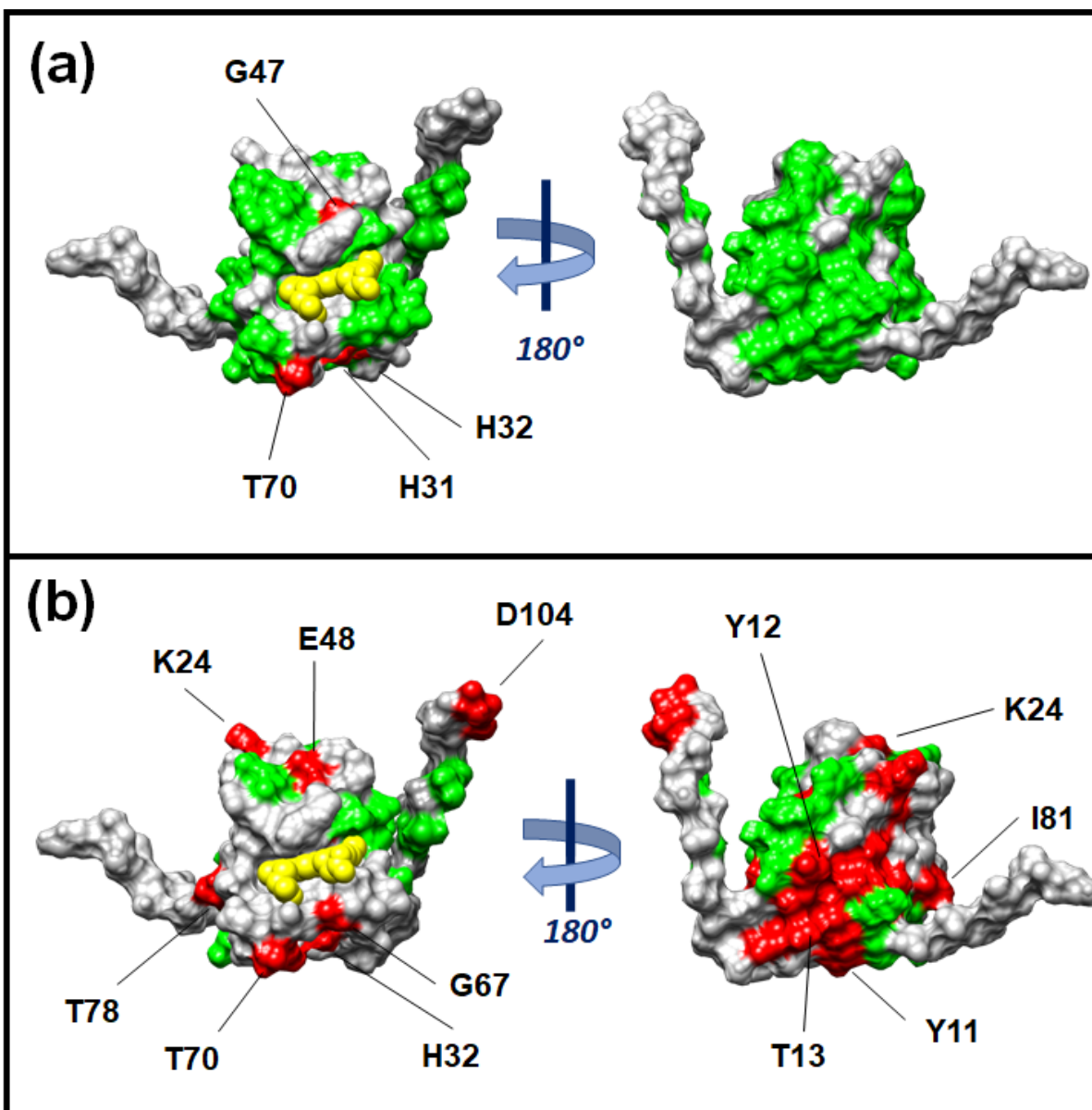


Figure S6. Two different views of space-filling representations of *cytb*₅ rotated by 180° with respect to each other for DMPC (a) and POPC:PS 8:2 (b) 4F-nanodiscs upon complex formation with an 0.8 molar amount of ligand-free CYP2B4; heme is depicted as yellow spheres. Grey and green indicate line broadening lower and higher than the average decrease of total line broadening, respectively; in red are the *cytb*₅ residues exhibiting extensive line broadening (with a decrease in peak height higher than average + 1σ as compared with free *cytb*₅).

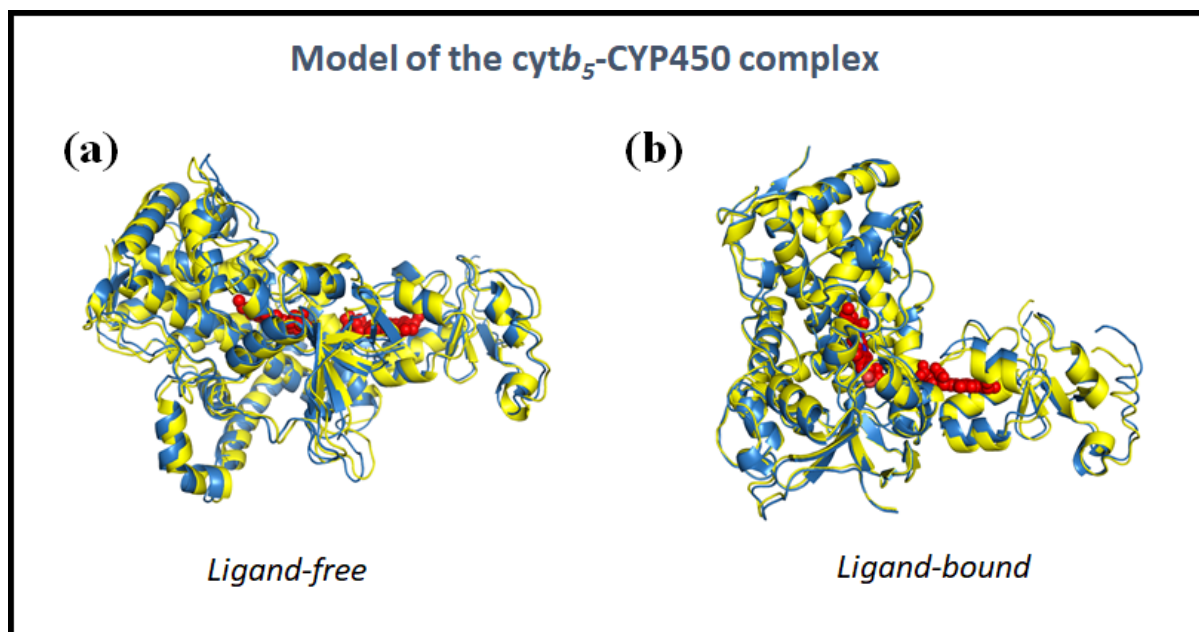


Figure S7. Models for the ligand-free (a) and ligand-bound (b) CYP2B4 complexed with *cytb*₅ in 4F-peptide nanodiscs, as obtained through HADDOCK 2.2 simulations. The schematics represent an overlap of the two complexes in DMPC (blue) and POPC-PS 8:2 (yellow) nanodiscs, showing negligible differences.

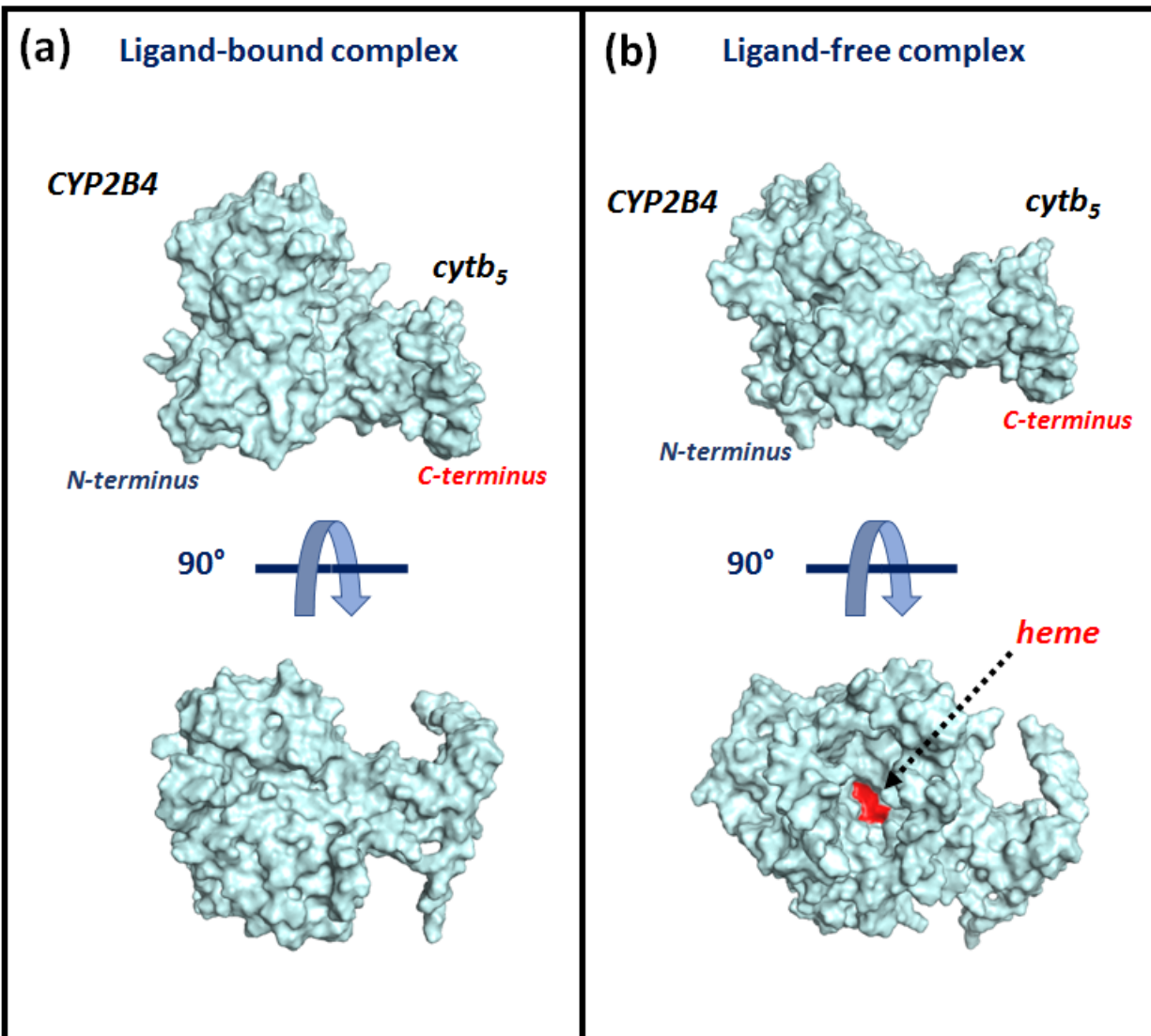


Figure S8. Comparison between ligand-bound (a) and ligand-free (b) CYP2B4-cyt_b₅ complexes in DMPC 4F-nanodiscs, as obtained from HADDOCK simulations. Rotation of the structures (bottom) show heme exposure to the solvent in ligand-free CYP2B4-cyt_b₅ complex. Similar results were obtained in the complex formed in POPC-POPS 8:2 nanodiscs (not shown).

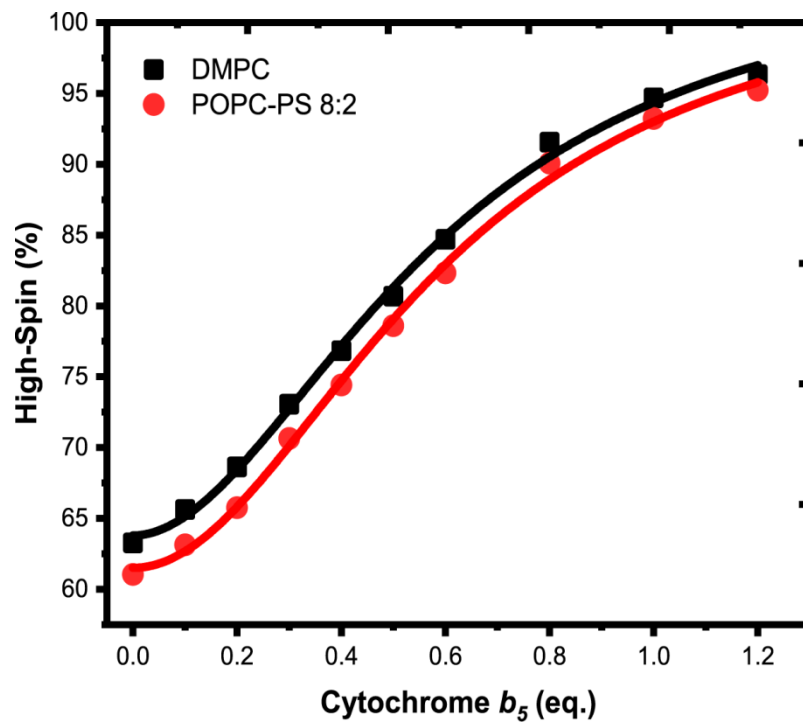


Figure S9. Fitting of the $cytb_5$ -induced spin-shifts titrations of CYP2B4 incorporated in DMPC (black) and POPC-PS 8:2 (red) 4F-nanodiscs, showing a sigmoidal profile for both nanodiscs preparations. The titration curve was fitted with eq. 1 (see Experimental Section in Supplemental Information).

Table S1. P450³Spin fractions of CYP2B4 reconstituted in 4F-nanodiscs with varying lipid composition: high-spin (HS), low-spin (LS), P420, and spectral equilibrium constant (K_S) using benzphetamine as ligand.

	HS (%)	LS (%)	P420 (%)	K_S (μM)
DMPC 100%	17	74	9	-
POPC 100%	26	61	13	13.8 \pm 0.6
POPC 80% POPS 20%	25	64	11	18.7 \pm 0.7
POPC 50% POPS 50%	33	60	7	17.0 \pm 0.9
POPC 20% POPS 80%	34	63	11	19.0 \pm 0.5
POPS 100%	33	56.	11	19.7 \pm 0.4

Table S2. Spin-state and Soret band shift in CYP2B4 titrated with *cytb*₅: maximum high-spin fraction (HS_{max}), peak maxima shift ($\Delta\lambda$), dissociation constant (K_D), and maximum high-spin fraction in the presence of substrate (HS_{max,s}).

	<i>+cytb</i> ₅ (no substrate)			<i>+cytb</i> ₅ + BP
	HS _{max} (%)	$\Delta\lambda$ (nm)	K_D (eq.)	HS _{max,s} (%)
DMPC	41	-8	0.81	96
POPC-PS 1:1	78	-11	1.40	-
POPC-PS 8:2	61	-7	0.83	95

Table S3. List of ambiguous and unambiguous restraints used in HADDOCK.

	Cytb₅	CYP2B4
Ambiguous active restraints	47, 48, 70, 71, 73, 74, 67	122, 126, 133, 135, 137, 139, 433
Unambiguous active restraints (Cytb₅- CYP2B4)	Asp65-Arg122, Val66-Arg122, Asp65-Lys433, Val66-Lys433	

Table S4. Energy statistics of lowest energy clusters of the CYP2B4 and *cytb*₅ complex in DPMC and POPC:POPS 8:2 4F-nanodiscs.

DMPC:

<i>HADDOCK score</i>	-132.0 +/- 8.3
<i>Cluster size</i>	199
<i>RMSD from the overall lowest-energy structure</i>	1.7 +/- 1.4
<i>Van der Waals energy</i>	-37.3 +/- 4.8
<i>Electrostatic energy</i>	-660.8 +/- 54.0
<i>Desolvation energy</i>	18.2 +/- 10.7
<i>Restraints violation energy</i>	192.6 +/- 22.03
<i>Buried Surface Area</i>	1621.7 +/- 98.1
<i>Z-Score</i>	0.0

POPC:POPS 8:2

<i>HADDOCK score</i>	-133.0 +/- 16.1
<i>Cluster size</i>	200
<i>RMSD from the overall lowest-energy structure</i>	0.6 +/- 0.3
<i>Van der Waals energy</i>	-40.7 +/- 2.4
<i>Electrostatic energy</i>	-685.1 +/- 103.8
<i>Desolvation energy</i>	23.4 +/- 5.5
<i>Restraints violation energy</i>	213.2 +/- 11.09
<i>Buried Surface Area</i>	1660.0 +/- 52.1
<i>Z-Score</i>	0.0

Table S5. Rate constants for second electron transfer in the presence/absence of benzphetamine (BP) as substrate.

	obs	λ_{\max}	A_1 (%)	k_1 (s^{-1})	A_2 (%)	k_2 (s^{-1})	A_3 (%)	k_3 (s^{-1})
<i>Solution</i>								
cytb₅	cytb ₅	422	-	-	-	-	97 ± 5	0.005 ± 0.0003
2B4²⁺	P450	438	25 ± 3	0.96 ± 0.2	34 ± 6	0.13 ± 0.04	41 ± 7	0.016 ± 0.005
2B4²⁺/BP	P450	438	-	-	40 ± 4	0.13 ± 0.05	60 ± 7	0.048 ± 0.004
2B4²⁺/BP	P450	438	n/a		~490 nm oxygen binding			
2B4²⁺/BP	P450	438	-	-	47 ± 5	0.15 ± 0.04	53 ± 4	0.053 ± 0.005
2B4²⁺ + cytb₅²⁺/BP	cytb ₅	422	50 ± 6	9.3 ± 0.7	4.0 ± 0.1	0.43 ± 0.21	46 ± 7	0.005 ± 0.0003
2B4²⁺ + cytb₅²⁺/BP	P450	438	62 ± 7	10.5 ± 1.5	18 ± 1.1	0.83 ± 0.18	20 ± 3	0.005 ± 0.001
<i>DMPC</i>								
cytb₅	cytb ₅	422	-	-	24 ± 3	0.29 ± 0.02	76 ± 4	0.003 ± 0.0003
2B4²⁺/BP	P450	438	-	-	10 ± 4	0.48 ± 0.05	90 ± 3	0.129 ± 0.03
2B4²⁺ + cytb₅²⁺/BP	cytb ₅	422	68 ± 5	11.3 ± 4	32 ± 5	0.08 ± 0.00	-	-
2B4²⁺ + cytb₅²⁺/BP	P450	438	72 ± 2	12.1 ± 4	27 ± 4	1.12 ± 0.20	-	-
<i>POPC:PS (8:2)</i>								
cytb₅	cytb ₅	422	-	-	52 ± 8	0.29 ± 0.04	97 ± 5	0.005 ± 0.0003
2B4²⁺/BP	P450	438	-	-	19 ± 4	0.75 ± 0.05	81 ± 2	0.117 ± 0.040
2B4²⁺ + cytb₅²⁺/BP	cytb ₅	422	55 ± 5	12.3 ± 3	45 ± 11	0.33 ± 0.10	-	-
2B4²⁺ + cytb₅²⁺/BP	P450	438	85 ± 5	12.7 ± 4	15 ± 2	1.82 ± 0.4	-	-

References:

- [1] S. Ahuja, N. Jahr, S.-C. Im, S. Vivekanandan, N. Popovych, S. V. Le Clair, R. Huang, R. Soong, J. Xu, K. Yamamoto, *Journal of Biological Chemistry* **2013**, *288*, 22080-22095.
- [2] U. H. Dürr, L. Waskell, A. Ramamoorthy, *Biochimica et Biophysica Acta (BBA)-Biomembranes* **2007**, *1768*, 3235-3259.
- [3] A. Bridges, L. Gruenke, Y.-T. Chang, I. A. Vakser, G. Loew, L. Waskell, *Journal of Biological Chemistry* **1998**, *273*, 17036-17049.
- [4] S. B. Mulrooney, L. Waskell, *Protein expression and purification* **2000**, *19*, 173-178.
- [5] A. S. Saribas, L. Gruenke, L. Waskell, *Protein expression and purification* **2001**, *21*, 303-309.
- [6] H. Kleinig, *The Journal of cell biology* **1970**, *46*, 396.
- [7] M. Zhang, R. Huang, R. Ackermann, S. C. Im, L. Waskell, A. Schwendeman, A. Ramamoorthy, *Angewandte Chemie International Edition* **2016**, *55*, 4497-4499.
- [8] J. B. Schenkman, I. Jansson, *Methods in Molecular Biology* **2006**, *320*, 11-18.
- [9] P. Strittmatter, S. F. Velick, *Journal of Biological Chemistry* **1956**, *221*, 253-264.
- [10] J.-P. Renaud, D. R. Davydov, K. P. Heirwegh, D. Mansuy, *Biochemical Journal* **1996**, *319*, 675-681.
- [11] D. R. Davydov, E. Deprez, G. H. B. Hoa, T. V. Knyushko, G. P. Kuznetsova, Y. M. Koen, A. I. Archakov, *Archives of biochemistry and biophysics* **1995**, *320*, 330-344.
- [12] M. Zhang, R. Huang, S.-C. Im, L. Waskell, A. Ramamoorthy, *Journal of Biological Chemistry* **2015**, *290*, 12705-12718.
- [13] T. Goddard, D. Kneller, *There is no corresponding record for this reference* **2014**.
- [14] S. Vivekanandan, S. Ahuja, S.-C. Im, L. Waskell, A. Ramamoorthy, *Biomolecular NMR assignments* **2014**, *8*, 409-413.
- [15] E. E. Scott, M. A. White, Y. A. He, E. F. Johnson, C. D. Stout, J. R. Halpert, *Journal of Biological Chemistry* **2004**, *279*, 27294-27301.
- [16] A. W. Schüttelkopf, D. M. Van Aalten, *Acta Crystallographica Section D: Biological Crystallography* **2004**, *60*, 1355-1363.
- [17] S.-C. Im, L. Waskell, *Archives of biochemistry and biophysics* **2011**, *507*, 144-153.